

Topology changes of the interface between two immiscible liquid layers by a rotating lid

Shuhei Fujimoto and Yasushi Takeda

Graduate School of Engineering, Hokkaido University, Kita-ku, Sapporo N13W8, Japan

(Received 13 April 2009; published 13 July 2009)

We report a deformation phenomenon occurring at the interface between two immiscible liquids. The two liquids are in a cylindrical container and set into motion by a rotating lid positioned above the interface. The upper liquid is more viscous than the lower and the difference in densities between the liquids is fairly small. As the rotational speed of the lid (Ω) is increased in small increments, the center of the interface rises and the height increases. Depending on Ω , the topology of the interface changes drastically. The shape of the interface depends strongly on Ω and also the volume fraction of the liquids. Some dynamical behavior of the interface accompanies the changes in topology: interfacial waves, the generation of droplets, and interfacial instability.

DOI: [10.1103/PhysRevE.80.015304](https://doi.org/10.1103/PhysRevE.80.015304)

PACS number(s): 47.55.N-, 47.32.Ef, 47.61.Jd

I. INTRODUCTION

When two immiscible liquids are layered, anomalous phenomena not found in single fluid systems may be generated, providing some vivid examples of nonlinear physics as visible actions [1]. In some instances, it appears in association with drastic interfacial deformations. For example, transient behavior (spin up) of immiscible liquids in a cylindrical container [2–4], a rod climbing effect in Newtonian fluids (two-liquid Taylor-Couette problem) [5], and a selective withdrawal (suction) [6–10] have been observed and investigated. In this Rapid Communication, we report topology changing phenomena found to occur at the interface between two immiscible liquids when the driving is due to the rotation of a disk. The experimental system is quite simple: a cylindrical container filled with two immiscible liquids and a rotating lid. For the case of the cylinder contains just a single fluid, the flow in the confined cylinder with a rotating end wall has been investigated in the context of vortex breakdown and mixing technology [11–16]. The subject of this Rapid Communication is a combined problem of the two-liquid dynamics and the confined swirling flow driven by a rotating disk. The change in the shape of the interface depends on the rotational speed of the lid (Ω). At relatively low Ω , the shape of the interface is a simple hump, which is very similar to the topology change of the interface found in selective withdrawal [6–10]. This is reasonable because the rotating disk draws fluid up along the axis of rotation and hence acts as a suction pump [17]. If Ω is sufficiently large, the shape of the interface shows further changes. In what follows, we describe the changes in the topology of the liquid interface and its dependence on two dimensionless quantities: the Reynolds number and the aspect ratio of the upper layer. The changes in the topology show chaotic or turbulent behavior at high Reynolds number and high aspect ratio. However, in this Rapid Communication we mainly focus on the steady-state flow behavior occurring at smaller Reynolds numbers.

II. EXPERIMENT

Figure 1 shows a schematic diagram of the experimental setup. The cylindrical container is made of transparent

acrylic resin with an inner radius (R) of 95 mm and a height (H) of 350 mm. The lid is also made of acrylic resin with an inner radius of 94.25 mm and a thickness of 5 mm. The rotational speed of the lid (Ω) was controlled by a brushless motor. A water jacket with a square cross section was employed to correct optical distortion. The lower layer is tap water and the upper layer is viscous silicone oil (kinematic viscosity is $\nu_u=130.0\text{--}145.0\text{ mm}^2/\text{s}$, slightly dependent on temperature). A difference in density between the liquids is about 3.5% and the liquid-liquid interfacial tension is $\gamma=42\text{ mN/m}$. Only the depth of the upper layer (H_u) was changed in ranges of $0.5R \leq H_u \leq 1.5R$: the depth of the lower layer (H_l) was fixed at $H_l=R$. The experimental results were organized by Reynolds number ($\text{Re}=\Omega R^2/\nu_u$) and aspect ratio of the upper layer (H_u/R). The shape of the interface was visualized by backlighting with a metal halide lamp. To obtain a clear profile, blue food dye was added to the water. The interfacial shape was recorded by a digital video camera from the side of the container with a frame rate of 30 fps and a shutter speed of 1/1000 s. In each run, the aspect ratio was fixed and Ω was incremented from low to high. When the rotating speed was changed, we let the system settle for a few minutes to allow transient motions to decay. Experiments were performed in ranges of Reynolds number between $0 \leq \text{Re} < 1000$.

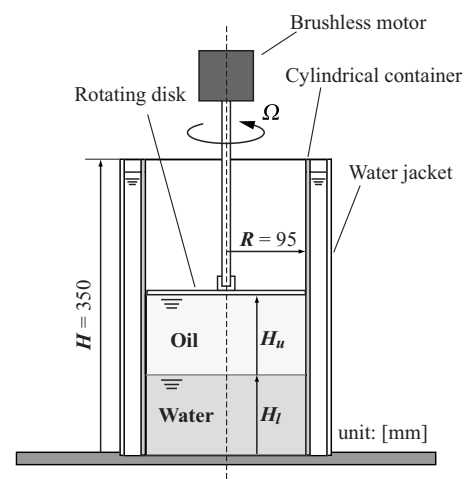


FIG. 1. Schematic diagram of the experimental setup.

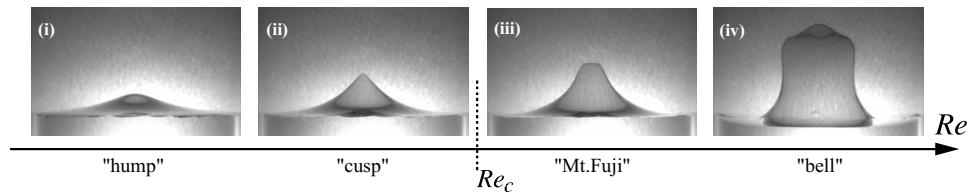


FIG. 2. Four typical shapes of interfacial deformation at $H_u/R=1.3$. From (i) to (iv) Re increases are called hump, cusp, Mt. Fuji, and bell, respectively. The Reynolds numbers are (i) 448, (ii) 531, (iii) 614, and (iv) 924.

III. RESULTS AND DISCUSSION

Four characteristic shapes of the interface were found and are shown in Fig. 2. We named these shapes “hump,” “cusp,” “Mt. Fuji,” and “bell” (The Mt. Fuji shape was so named due to its resemblance to Mt. Fuji, Japan.) These shapes are axisymmetric and stationary and appear without hysteresis. Also, the deformed interface rotates in the same direction as the rotating lid. The center of the interface rises and the magnitude of the upheaval increases with increases in Re . At a relatively small Re , the shape of the interface is a simple hump. As the Re increases, a cusp shape appears at the center of the interface; where the tip becomes sharp. Then with a further increase in Re , Mt. Fuji appears: the tip of the cusp changes to a flat surface at the top of the interface. With still further increases in Re , the shape we call bell appears. This means that the growth of Mt. Fuji is in the radial direction rather than in the axial direction; in other words, the liquid column thickens with increasing Re . In this bell shape, the interface has constricted part. In addition, a small hump forms on top of the flat surface (the summit of Mt. Fuji) and it grows with increasing Re . A sequence of these topology changes is shown in Fig. 3. The lines indicate the profile of the interfacial height as a function of radial location [$h(r)$]. $h(r)=0$ means the height of the interface at rest state. For the

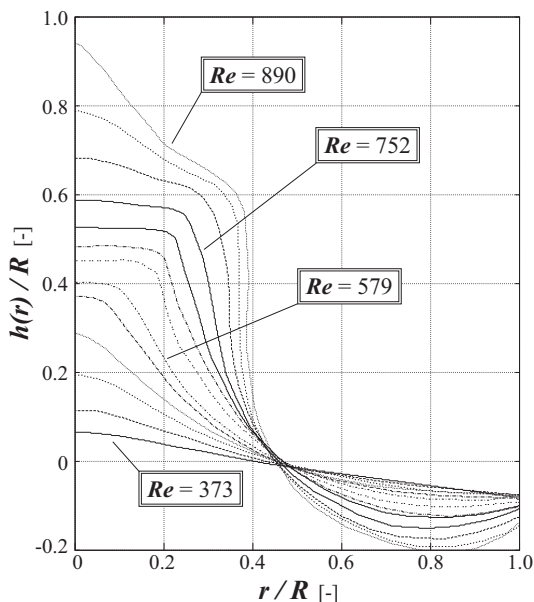


FIG. 3. Profiles of deformed interface at $H_u/R=1.2$. At $r/R=0$, from bottom to top $Re=373, 414, 462, 497, 545, 579, 642, 676, 711, 752, 814, 855, 890$, respectively.

aspect ratio of $H_u/R=1.2$, the 12 profiles were acquired from the image by reading the location of the interface for the 12 Reynolds numbers. Each profile was classified in the above-noted four shapes as follows: 373–462 are in hump, 497 is in cusp, 545–676 are in Mt. Fuji, and 711–890 are in bell. These are the classification by visual observation. Because of the constriction of the interface in bell, $h(r)$ has multiple values at a certain range of r . To assess the changes in the interfacial shapes quantitatively, we employed two quantities. One is the height of the center of the interface [$h_0:h_0=h(0)$ in Fig. 3] and the other is the “half-width at half maximum” (HWHM) of the interfacial shape. Figure 4 shows the changes in h_0 and HWHM with respect to Re . We defined HWHM as a radial location at a half height of the maximum difference of interface height (inset of Fig. 4). The curve of HWHM is a minimum for the cusp; the local minimum is the point where the cusp turns into Mt. Fuji, and after this point the direction of the growth changes as noted above. We estimated a critical Reynolds number (Re_c) for the transition from cusp to Fuji by a linear least-squares approximation (Fig. 4). The curve of h_0 also changes its gradient at Re_c . The change in the gradient indicates a qualitative shift of the topology of the interface.

Figure 5 shows a phase diagram for the interfacial topologies and pictures of some characteristic shapes. The top boundary of the diagram indicates a constraint or upper bound of the experiment. We observed three different types of constraints. First, there is a restriction in the growth of the height of the interface (■ in Fig. 5): the center height h_0 increases with Re and it cannot exceed H_u due to the lid. Second, there is a local instability (▼): in a certain range of

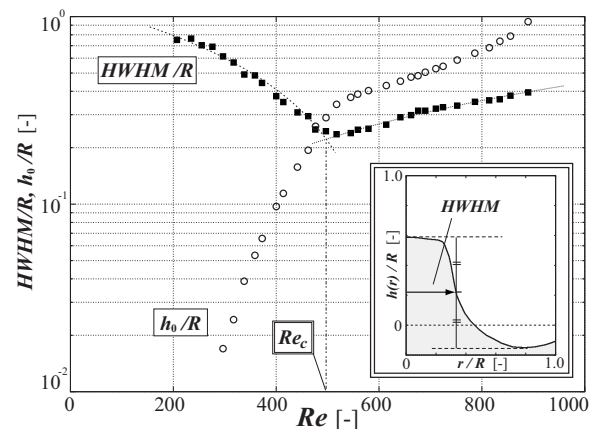


FIG. 4. Changes in HWHM and center height $h_0 [=h(0)]$ in Fig. 3 at each Re at $H_u/R=1.2$. The inset illustrates the definition of HWHM.

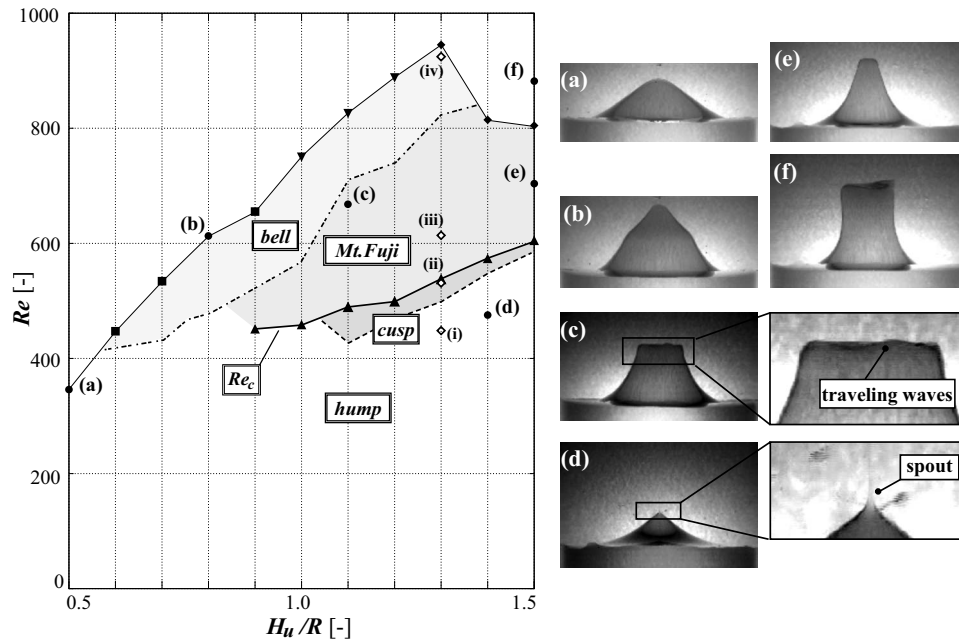


FIG. 5. Phase diagram for the deformed shape of the interface. (a) $H_u/R=0.5$ and $Re=346$. At this aspect ratio, the hump state is maintained until the center of the interface attaches to the rotating lid. (b) $H_u/R=0.8$ and $Re=613$. Although this state is classified as bell, the radial gradient of the interface is small compared to the bell for high H_u/R [e.g., Fig. 2(iv)]. (c) $H_u/R=1.1$ and $Re=669$. Traveling waves arise at the rim of the top flat surface. (d) $H_u/R=1.4$ and $Re=476$. A spout [10] is formed at the tip of the hump. (e) $H_u/R=1.5$ and $Re=703$. An elongated Mt. Fuji. (f) $H_u/R=1.5$ and $Re=860$. The deformed interface loses axial symmetry and starts to oscillate horizontally.

H_u/R , small droplets are generated periodically at the tip of the bell-shaped interface. Third, there is a global instability (\blacklozenge): at relatively large H_u/R , the deformed interface loses axial symmetry and starts to oscillate horizontally [Fig. 5(f)]. The global instability was most likely due to wobbling of the rotating lid or eccentricity of the container. The dashed lines in the diagram are the boundaries of the interfacial shapes determined visually. The black triangles (\blacktriangle) with a solid line are the lower boundary of Mt. Fuji and indicate Re_c . The four characteristic shapes in Fig. 2 ($H_u/R=1.3$) are also plotted in Fig. 5 (\blacklozenge). The shape of the interface depends strongly on H_u/R . If the aspect ratio is sufficiently small ($H_u/R < 0.6$), the phases except for hump never set in. At $H_u/R=0.5$, the center of the interface reached the upper rotating disk before a further change in topology [Fig. 5(a): $Re=346$]. With an increase in H_u/R , the diversity of the interfacial shapes is promoted and the transitions of the shapes are delayed. Additionally, the *complexity* of the shape of the interface increases. To compare Figs. 2(iv) and 5(b): $H_u/R=0.8$ and $Re=613$ [or Figs. 2(iii)–5(e): $H_u/R=1.5$ and $Re=703$], though both of them are classified in bell (Mt. Fuji), the case of high aspect ratio is more complex; the curvature of the profile changes sharply or the height function $h(r)$ is multivalued. Above a certain level of the aspect ratio ($0.9 < H_u/R$), the traveling wave appears in Mt. Fuji at the rim of the top flat surface [Fig. 5(c)]. Another remarkable feature is the entrainment of lower liquid [Fig. 5(d)]: at relatively high H_u/R , the lower liquid is entrained and brought up along the center axis. The top of the hump is elongated (formation of “spout” [10]), then a small amount of lower liquid is torn apart to form tiny drop, which rises into the upper liquid.

IV. CONCLUSIONS

Topology changes of the interface between two immiscible liquid layers induced by a rotating lid were studied. We found four types of typical shape of the interface: hump, cusp (the center of the hump sharpens), Mt. Fuji (the tip of the cusp is flattened), and bell (the shape of the interface has constriction part or a small hump arises at the top of the interface). These shapes appear with increases in the Reynolds number. These shapes are basically axisymmetric and stationary and appear without hysteresis. We defined a critical Reynolds number for the transition from cusp to Mt. Fuji: the direction of the growth of the shape changes at the critical value. The shape of the interface also strongly depends on the aspect ratio of the upper layer. The diversity of the shapes of the interface is promoted with an increase in the aspect ratio. This is because the *degree of freedom* of the flow in the upper layer increases with an enlargement of the aspect ratio. The same tendency in the diversity is found in the phase diagram of a single fluid layer [11].

Some remarkable features were also found: generation of the interfacial waves (a kind of spontaneous symmetry breaking), formation of droplets (singularity of the interface), and interfacial instability. Due to these interfacial dynamics, this confined two-layer system has potential applications in the mixing of immiscible liquids and in emulsification technology. At the same time, for quantitative description of the phase diagram, other configuration parameters such as a height (aspect ratio) of lower layer, ratio of density and viscosity, and/or interfacial tension between two layers may have to be involved.

- [1] D. D. Joseph and Y. Y. Renardy, *Fundamentals of Two-Fluid Dynamics* (Springer-Verlag, New York, 1993), Parts I and II.
- [2] T. G. Lim, S. Choi, and J. M. Hyun, *J. Fluids Eng.* **115**, 324 (1993).
- [3] K. Y. Kim and J. M. Hyun, *J. Fluids Eng.* **116**, 808 (1994).
- [4] T. Sugimoto and M. Iguchi, *ISIJ Int.* **42**, 338 (2002).
- [5] D. Bonn *et al.*, *Phys. Rev. Lett.* **93**, 214503 (2004).
- [6] C. S. Yih, *Dynamics of Non-homogeneous Fluids* (McMillan, New York, 1965), p. 204.
- [7] J. R. Lister, *J. Fluid Mech.* **198**, 231 (1989).
- [8] I. Cohen and S. R. Nagel, *Phys. Rev. Lett.* **88**, 074501 (2002).
- [9] I. Cohen, *Phys. Rev. E* **70**, 026302 (2004).
- [10] S. C. Case and S. R. Nagel, *Phys. Rev. Lett.* **98**, 114501 (2007).
- [11] M. P. Escudier, *Exp. Fluids* **2**, 189 (1984).
- [12] A. Spohn, M. Mory, and E. J. Hopfinger, *Exp. Fluids* **14**, 70 (1993).
- [13] D. L. Boyer, P. A. Davies, and Y. Guo, *Fluid Dyn. Res.* **21**, 381 (1997).
- [14] R. J. Munro and P. A. Davies, *Fluid Dyn. Res.* **38**, 522 (2006).
- [15] P. Yu *et al.*, *Phys. Fluids* **18**, 117101 (2006).
- [16] P. Yu *et al.*, *Phys. Fluids* **20**, 087103 (2008).
- [17] G. K. Batchelor, *An Introduction to Fluid Dynamics* (Cambridge University Press, Cambridge, 1967), p. 290.